Pergamon

Bioorganic & Medicinal Chemistry 8 (2000) 1331–1342

BIOORGANIC & MEDICINAL CHEMISTRY

Observations on the Covalent Cross-Linking of the Binding Domain (BD) of the High Mobility Group I/Y (HMG I/Y) Proteins to DNA by FR66979

Scott R. Rajski and Robert M. Williams*

Department of Chemistry, Colorado State University, Fort Collins, CO 80523, USA

Received 29 November 1999; accepted 3 February 2000

Abstract—FR66979, a drug closely related to the mitomycin C class of antitumor antibiotics, is shown to covalently cross-link DNA to the DNA-binding domain of the High Mobility Group I/Y (HMG I/Y) DNA-binding proteins in the minor groove.

Introduction

DNA interstrand cross-linking agents are widely regarded as among the most significant chemotherapeutic agents available.[1–3] The potent antitumor and antibacterial properties exhibited by such agents is attributed to their capacity to covalently bind the two strands of duplex DNA thus abrogating events of biological importance such as transcription and DNA replication.[4] The presence of two reactive sites within such molecules hints that other manifolds may exist by which such agents may express biological activity; monoalkylation of biomacromolecules and nucleic acid–protein cross-linking being the most likely. Tenacious cellular DNA repair mechanisms dictate that DNA monoalkylation is significantly less important in the expression of therapeutic activity.[5] However, DNA–protein cross-linking can in principle, be presumed to result in lesions of vastly greater importance than monoalkylation adducts. The importance of DNA–protein cross-links relative to that of DNA–DNA interstrand cross-links is not yet known since, research aimed at the elucidation of DNA–protein cross-linking mechanisms has been hampered by the generally lower yields of such adducts relative to the interstrand events and the radically more complex and diverse structural possibilities inherent to nucleic acid–protein cross-links.

FR900482 (**1**) and FR66979 (**2**) are recently discovered antitumor antibiotics that were obtained from fermentation harvests of *Streptomyces sandaensis* No. 6897 at the Fujisawa Pharmaceutical Co. in Japan (Fig. 1).[6–9] The clinical candidates FK973 (**3**) and FK317 (**4**), both semi-synthetically derived from FR900482, have shown highly promising antitumor activity in human clinical trials. FK317 is now in advanced human clinical trials in Japan[10] and holds significant promise to replace the structurally related and widely used antitumor drug mitomycin C (MMC, **6**).[11]

Early biological studies conducted at Fujisawa Co. revealed that both FR900482 and FK973 effected the formation of DNA interstrand cross-links and DNA–protein cross-links of undefined constitution in L1210 cells.[7,9] In contrast to MMC,[11] the Fujisawa drugs do not cause oxidative single strand scission of DNA. Particularly notable is that FK317 and FK973 are significantly less host-toxic than mitomycin C and are ca. 3-fold more potent. Moreover, these acetoxy derivatives in addition to the parent compound FR900482 are active against multidrug-resistant P388 cells.[10c]

It is well established that MMC is reductively activated both in vitro and in vivo to provide an electrophilic mitosene via the bioreductive in situ formation of a semi-quinone radical anion species. The mitosene derived from reductive activation of MMC cross-links DNA, preferentially at $^{5'}$CpG$^{3'}$ sites.[12] However, formation of the potent *bis*-electrophilic mitosene, is accompanied by non-specific oxidative damage to DNA and presumably, other healthy cellular macromolecules. This is the result of superoxide production resulting from adventitious reduction of molecular oxygen by the

*Corresponding author. Tel.: +1-970-491-6747; fax: +1-970-491-1801; e-mail: rmw@chem.colostate.edu

0968-0896/00/$ - see front matter
PII: S0968-0896(00)00078-X

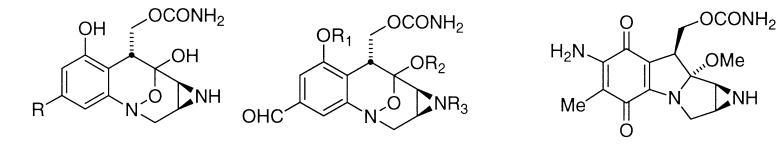

1, FR-900482, R = CHO
2, FR-66979, R = CH_2OH
3, FK-973, R_1= R_2 = R_3 = Ac
4, FK-317, R_1 = Me, R_2 = R_3 = Ac
5, FR-70496, R_1 = Me, R_2 = H, R_3 = Ac
6, mitomycin C (MMC)

Figure 1.

obligate semi-quinone radical anion intermediate enroute to the mitosene; subsequent Haber–Weiss/Fenton cycling produces hydroxyl radical and related diffusable oxidants capable of causing non-selective tissue damage. The low host toxicity of FK317 in clinical trials relative to MMC may be correlated to the incapacity of this agent to cause indiscriminate oxidative damage to DNA and other healthy cellular targets. Since FK317 and MMC both share the ability to cross-link DNA, it is very clear that the lack of oxidation chemistry inherent in FK317 has not at all compromised its efficacy as an antitumor drug relative to MMC.

It has been demonstrated that FR900482 (and by analogy, FR66979, FK973 and FK317) undergoes reductive activation in vitro to form the reactive mitosene derivative **9** (Scheme 1) which preferentially cross-links duplex DNA at $^{5'}$CpG$^{3'}$ steps.[13–15] The mechanism of reductive activation involves the thiol-mediated two-electron reduction of the N–O bond in the presence of trace Fe(II) salts generating the transient ketone **7** which rapidly cyclizes to the carbinolamines **8**. Expulsion of water has been inferred as the rate-determining step enroute to the electrophilic mitosene.[14d]

Among the initial reports concerning the biological activity of the FR900482 antitumor antibiotics was the finding that these agents induce DNA–protein cross-links.[7,9] The application of alkaline elution methods indicated the time-dependent formation of such cross-links in murine leukemia L1210 cells.[7,9] However, the isolation and characterization of such cross-links was not reported. More significantly, the absence of careful structural elucidation of the DNA–protein adducts formed by mitomycin C and the structurally related pyrrolizidine alkaloids has persisted for some 30 years.[16]

Given the structural analogy of the mitomycins and the FR drugs, elucidation of the pathway to these lesions was deemed a highly significant undertaking.

The size and secondary structure of most proteins mandate that DNA–protein interactions occur primarily in the more sterically accessible major groove of duplex DNA.[17] Alternative minor groove sequence-specific binding motifs are much less common and are typically associated with AT rich sequences.[17] This is the result of several factors: specific hydrogen-bonding to adenine and/or thymine bases; the greater negative electrostatic potential in such sequences; the narrowing of the groove in AT-rich regions and oligo(dA) tracts, and the complementarity between groove and ligand curvature.[18]

Perhaps the most well studied of the minor groove protein–DNA motifs are the HMG proteins. The HMG I proteins belong to the 'high mobility group' (HMG) class of mammalian chromatin proteins ubiquitous in higher eukaryotes.[19,20] These non-histone chromosomal proteins are preferentially expressed in undifferentiated, neoplastically transformed, and rapidly proliferating cells.[20] HMG nucleoproteins may be divided into three groups based on their size, sequence homology and DNA binding properties: HMG-1/-2, HMG-14/-13 and HMG-I/Y.[21,22] Of the three subclasses, HMG I is the most heavily explored. With the exception of an internal 11 amino acid deletion, HMG-Y is identical to HMG-I.[20]

Like other HMG proteins, HMG-I has been implicated in transcriptional regulation and in the proper maintenance of structure and expression of chromatin.[11,23] Bearing both a DNA-binding domain and a negatively charged surface (at the C-terminus) these proteins fulfill the requirements of a Ptashne-type activator protein.[19]

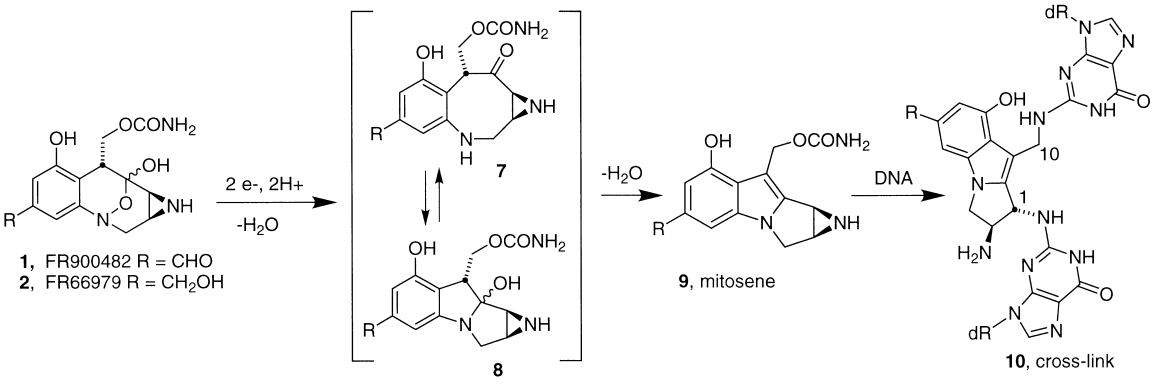

1, FR900482 R = CHO
2, FR66979 R = CH_2OH
2 e-, 2H+
$-H_2O$
7
8
$-H_2O$
9, mitosene
DNA
10, cross-link

Scheme 1.

Therapeutically significant is that high HMG-I levels are a consistent feature of rat and mouse malignant cells and have been suggested as a protein marker for neoplastic transformation and metastatic potential.[24] HMG-I(Y) are distinguished from other HMG proteins by their ability to specifically bind double-stranded DNAs containing sequences of at least four continuous AT-bases (ideally, 5′-AATT-3′).[25] Binding is sensitive to the local conformation of the minor groove of DNA instead of the specific nucleotide sequence, although sequence-dependent DNA conformation clearly plays a role. Binding affinity and specificity results from three homologous TPKRPRGRPKK DNA-binding domains (BD).[24,26] Molecular modeling and NMR structural data has revealed that the binding domain (**BD 11**; Fig. 2) possesses a crescent shape reminiscent of netropsin and distamycin resulting from the predominantly *trans*-prolines at either end of the PRGRP palindrome.

Binding to the minor groove of A-T-rich DNA occurs via replacement of the inner spine of hydration by the donation of bifurcated hydrogen bonds from the appropriately placed amide NH residues in the peptide backbone.[24,26] Additionally, the non-specific ionic interactions of lysine and arginine with the anionic DNA backbone are responsible for most of the DNA binding energy.[24] This is consistent with the protein's salt-dependent DNA-binding affinity.

The 'AT-hook' motif inherent to TPKRPRGRPKK results from the synergism of the N-terminus TPK hook and the proline-induced crescent conformation of the RPRGRPKK fragment.[23] The N-terminal 'hook' results from an Asx-turn resulting partly from intramolecular hydrogen bonding between the threonine hydroxyl and the lysine-to-proline amide hydrogen.[23,27] Reeves and Nissen have shown that substitution of alanine for threonine at this position results in retention of the hook motif and analogous DNA-binding affinities.[23] As such, the main contributor to the hook motif observed is proposed to be the neighboring proline which effects pronounced kinking of the N-terminus. This kink specifically orients the peptide amide one residue ahead of the proline into a strong hydrogen bond in the minor groove, most likely with the N^3 of 2′-deoxyadenosine or the O^2 of 2′-deoxythymidine. The intramolecularly stabilized tripeptide fits tightly into the wide minor groove of AT/GC junctions and has been implicated as a major factor in DNA binding by TPKRPRGRPKK.[23,24]

Due to the significance of the HMG-I(Y) proteins and the provocative preliminary report of DNA-protein cross-link formation mediated by FK973,[9] we have examined the capacity of the simple congener, FR66979 to mediate cross-link formation between duplex DNA and the binding domain of the HMG-I(Y) proteins.[28] We report herein the demonstration of DNA-peptide cross-link formation by FR66979 (**2**); this represents the first demonstration of mitosene-based cross-linking of DNA to a DNA-binding protein motif.[29]

Results and Discussion

Wemmer and co-workers had shown by ^{1}H NMR analysis that the short binding domain peptide fragments derived from HMG-I/Y proteins (TPKRPRGRPKK; PRGRPKK; and PRGRP) bind specifically to the central AT sites of the self-complementary oligonucleotides 5′-CGCAAATTTGCG-3′ and 5′-CGCGAATTCG-CG-3′.[30] The arginine side chains of each peptide protrude deep into the minor groove (Fig. 3) in a fashion similar to that known for the antibiotic netropsin.[26] The PRGRP run of each peptide bound specifically to the 5-AAATTT-3 region of the DNA duplexes examined. Notably, peripheral segments of the longer peptides associate with the flanking CG base pairs.[26] These contacts have been further elaborated upon vis-à-vis the solution structure of DNA-bound human HMG-I(Y) (Fig. 3).[30] The minor groove nature of these peptide–DNA interactions and the known amenability of the FR drugs to react within the minor groove of DNA suggested that this motif may be one of potential significance with respect to FR-mediated DNA–protein cross-linking reactions.

The ^{1}H NMR-derived structure for peptide–DNA binding revealed that one of the two arginines within the site-recognizing PRGRP sequence came within close proximity to the exocyclic N^2 amine of the 5′-AATT-3′ abutted dG.[26] Further, minimization of this complex (coordinates courtesy of Wemmer and co-workers) with the FR66979-derived mitosene at a dG mono-alkylation

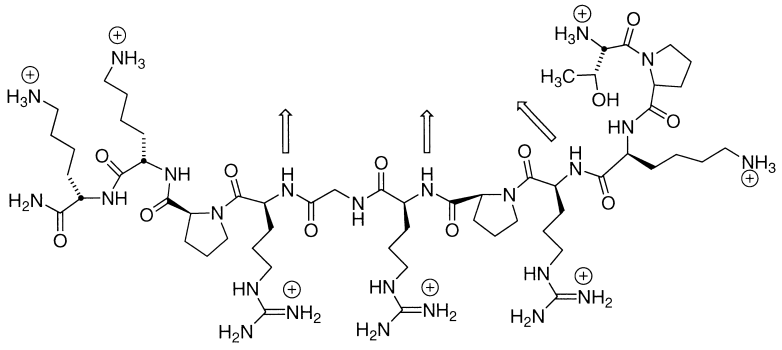

11, *HMG I Binding Domain (BD) peptide*

Figure 2.

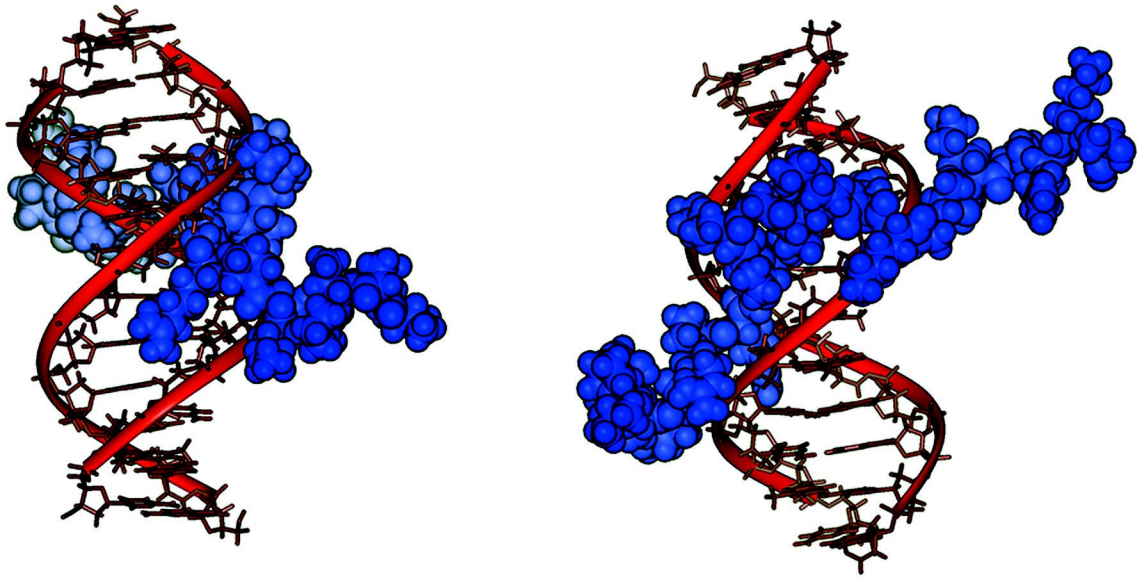

Figure 3. Two views of the human HMG-I(Y) protein bound to DNA. Coordinates were downloaded from the Protein Data Bank and manipulated with InsightII software. Both angles of the ^{1}H NMR structure reveal tight DNA–protein contacts deep within the minor groove (from ref 30).

site flanking the 5′-AATT-3′ showed minimal distortion of the DNA duplex by the bound drug (Fig. 4). Close examination revealed the mitosene-derived electrophilic C10 to be ~2 Å from one of the guanidines of the two palindromic arginines of PRGRP. An interesting feature revealed by the modeling involved the disposition of the amino group at N^2 (from aziridine ring opening of reductively activated **2**). When docked to a cross-linkable $^{5'}$CpG$^{3'}$ site, this amine is within 2 Å of the exocyclic N^2 of the opposing G residue. Presumed repulsive interactions between the two thus suggested that a $^{5'}$GpG$^{3'}$ mono-alkylation site could be interesting to examine since it positions the amino group in perfect H-bonding distance (2–4 Å) of the carbonyl on the opposing C-residue. This net conversion of a repulsive interaction to an attractive one could likely facilitate formation of a covalent DNA–peptide lesion. Thus, efforts focused on DNA substrates which poised $^{5'}$CpG$^{3'}$ (interstrand cross-linking sites) or $^{5'}$GpG$^{3'}$ (monoalkylation sites) on either side of the HMG binding sequence $^{5'}$AAATTT$^{3'}$ (Fig. 5). Another consideration specific to those duplexes bearing cross-linkable $^{5'}$CpG$^{3'}$ sites involved the potential for inadvertant interstrand cross-link formation; leading to difficulties in visualizing, via electrophoretic techniques, the HMG–DNA cross-link of interest. To avoid this complicating side reaction, the nucleotide deoxyinosine was incorporated complementary to the cytosine of $^{5'}$CpG$^{3'}$ sequences (templates **A** and **B**, Fig. 5).

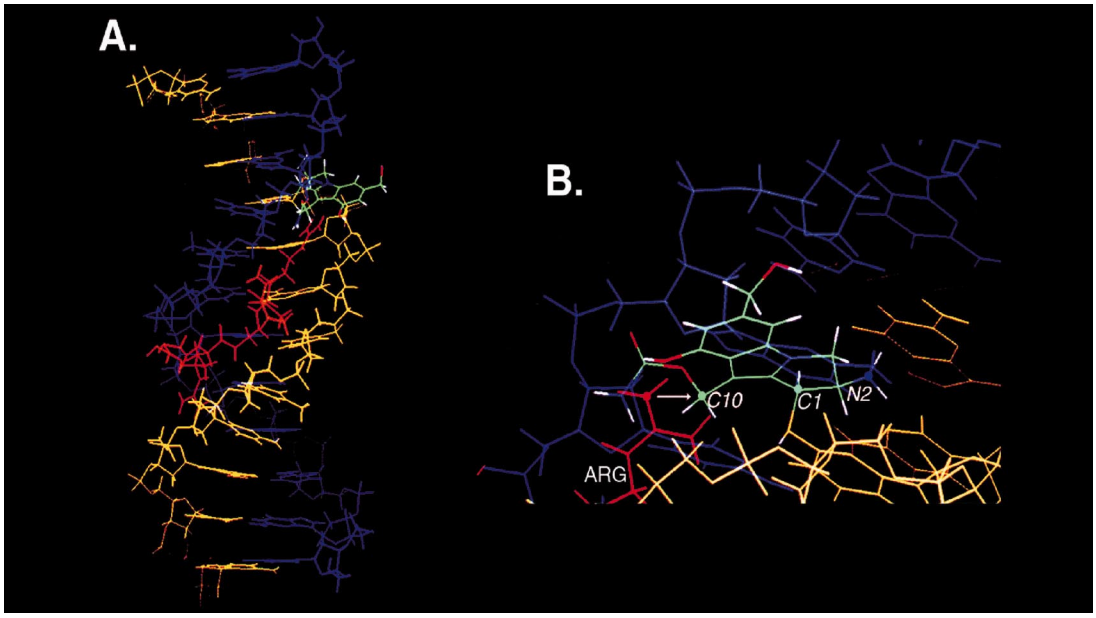

Figure 4. Molecular mechanics calculations for the proposed DNA–drug mono-alkylation adduct. Panel A depicts the full-length DNA–FR–HMG complex. The immediate vicinity of the FR-modified complex is shown in panel B. Notably, the FR66979-derived mitosene (green) is covalently attached via C1 to N^2 of the dG residue of the right side strand (yellow). This allows close approach of an HMG binding domain arginine (red) to the mitosene C10.[31] The distance denoted by the white arrow is approximately 2.3Å.

Figure 5.

In the area of model peptide design we had observed that incorporation of either a cysteine or *N*-ϵ-dansyl-L-lysine at the N-terminal side of the TPK sequence gave rise to complicating drug-independent covalent cross-linking to the DNA duplex template **A**. These N-terminal moieties were originally intended to allow for more facile identification and purification of peptide–drug–DNA adducts than was expected for unsubstituted peptide **BD 11**. Despite the undesired chemistry witnessed with these variants of **BD 11**, these studies showed quite clearly that a DNA–peptide complex would be easily detectable and separable from other reaction products via simple gel electrophoresis techniques. We thus explored the use of the simple HMG peptide **BD 11** (Fig. 2). As discussed above, those cases in which the $^{5'}$AAATTT$^{3'}$ of the DNA recognition site is flanked to the 5′ side by a FR66979-monoalkylated dG were expected to most readily react with an arginine side chain of PRGRP. Efforts involving the simultaneous reaction of FR66979, DTT, **BD 11** and template **A** failed, however, to afford discernible gel-shifted material. This was attributed to one of two phenomena: (a) either the peptide shielded the DNA from alkylation via tight binding; or (b) the peptide underwent alkylation with comparable or better efficiency than the DNA substrate. Given the salt dependence of BD peptide binding to $^{5'}$AAATTT$^{3'}$, the latter hypothesis was favored. In stark contrast to early efforts using dansylated or thiolated HMG peptides, the formation of drug-independent peptide–DNA complexes was not apparent in reactions of template **A** with **BD 11**.

An alternative approach aimed at assessing the ability of FR66979 to covalently cross-link **BD 11** to any of the templates **A**–**C** involved a stepwise strategy. It was believed that initial duplex alkylation followed by rigorous purification and desalting would give rise to a species capable of peptide binding. This approach proved successful, particularly using the duplex substrate template **A**.

Monoalkylation of template **A** followed by repeated EtOH precipitation and Sephadex G-50 size exclusion chromatography, yielded the mixture of native and alkylated substrate in good yields (≥90%). Of the radiolabeled material isolated, 20–40% had suffered monoalkylation. Dilution of the alkylated substrate to a concentration of 20 pmol/μL (20 μM in duplex) in 10 mM Tris (pH = 8.0) yielded the desired DNA stock solution. Equal volumes of this stock solution and 10 μM, 100 μM, 1 mM, and 10 mM solutions of **BD 11** in DDH_2O were incubated at 37 °C for 12 h in glass-lined vials. Despite the use of glass-lined vials for the peptide reactions, the vast majority of material was unrecoverable for reactions in which the overall concentration of peptide exceeded 50 μM.[32]

Optimal amounts of gel-retarded, drug-dependent material were obtained in reactions wherein the overall peptide concentration was 50 μM. From these reactions it appears that a ratio of FR66979-alkylated DNA:**BD 11** of 1:5 was optimal for formation of the observed gel-shift. Differential radiolabeling of either strand of template **A** revealed that cross-link formation was not relegated exclusively to ODN **12** as originally envisioned (Fig. 6). The observation that residues other than the anticipated dG immediately to the 5′ side of $^{5'}$AAATTT3′ underwent drug-mediated DNA-peptide cross-linking represented a surprising, but important result. The incorporation of inosine (in ODN**12′**) across from the $^{5'}$CpG$^{3'}$ run proximal to $^{5'}$AAATTT$^{3'}$ of DNA **12** was anticipated to facilitate identification of the HMG-DNA cross-link by abrogating interstrand cross-linking and allowing the formation of the peptide–DNA cross-link. As such, the argument that the template **A** scenario was not representative of a naturally occurring situation was certainly valid and difficult to refute. Drug-dependent peptide cross-linking to both strands of template **A** thus demonstrates the generality of this motif.

To confirm the covalency of the adduct formed, ligand/DNA-exchange reactions were performed. The purified radiolabeled complexes of **BD 11** with substrate **12** and substrate **12′** were incubated with unlabeled competitor template **A**. Incubation of each drug-mediated complex with increasing amounts of unlabeled competitor DNA template **A** at 37 °C for 24 h. failed to exchange **BD 11** from either radiolabeled strand. Complete retention of each radiolabeled complex was observed with a > 1000-fold molar excess of unlabeled competitor template **A** (Fig. 7). This supported the belief that the peptide–DNA

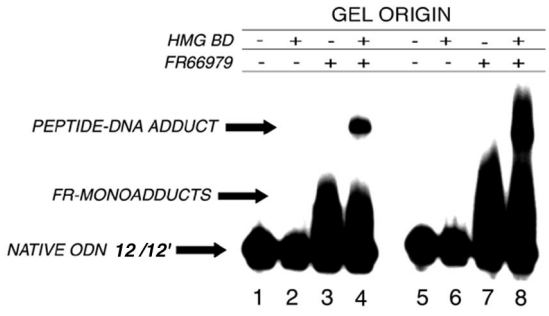

Figure 6. DNA–protein cross-linking by reductively activated **2**. All reactions were incubated 37 °C in 5 mM Tris (pH = 8.0) for 12 h. All DNA substrates were desalted by Sephadex G-50 chromatography and subsequently EtOH precipitated prior to peptide addition. **Lanes 1–4**, reactions of template **A** (5′-end-labeled **12′**). **Lanes 5–8**, reactions of template **A** (5′-end-labeled **12**). **Lanes 1**, **5**, template **A** standards. **Lanes 2, 6**, 50 μM **BD 11** + DNA controls. **Lanes 3, 7**, DNA + FR66979/DTT controls. **Lanes 4, 8**, FR66979 alkylated template **A** + 50 μM **BD 11**.

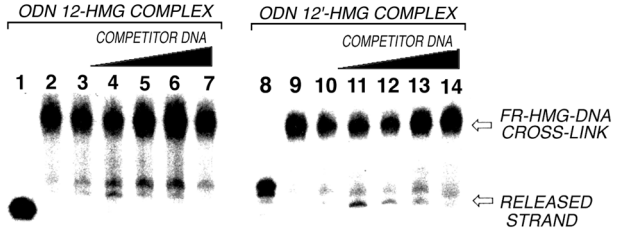

Figure 7. DNA exchange reactions of unlabeled template **A** with **ODN 12** and **ODN 12′** complexes with HMG BD peptide **BD 11**. All complexes were obtained after purification from FR66979 reactions and subsequent 3′-end labeling with polynucleotidyl transferase. **Lane 1**: standard template **A**. **Lane 2**: **BD 11** complex with **ODN-12** control. **Lane 3**: **BD 11-ODN 12** complex incubation control (no unlabeled DNA included); **Lanes 4–7**: **BD 11**–**ODN 12** complex incubated with 0.25, 2.5, 25, and 250 μM unlabeled template **A**, respectively. **Lane 8**: template **A** control (**ODN-12′** radiolabeled), **lane 9**: **ODN 12′-BD 11** complex (no incubation); **Lane 10**: **BD 11** complex with **ODN-12** incubation control (no unlabeled DNA), **Lanes 11–14**: **BD 11**–**ODN 12** complex incubated with 0.25, 2.5, 25, and 250 μM unlabeled template **A**, respectively.

complexes formed were covalent in nature and not due to simple non covalent interactions.

Verification of ligand-exchange data was sought via negative ion electrospray mass spectral analysis of the 20% DPAGE purified complex. Numerous high mass signals (much higher than for either DNA strand alone or their peptide-bound congeners) were obtained in the m/e = 12,700–12,950 Da range (Fig. 8). The calculated mass of an **ODN 12**–drug–**BD 11** conjugate is 12,721.3 Da, assuming that the covalencies involved are relegated to the mitosene 1 and 10 positions. Additionally, this mass takes into account that the peptidic portion (corresponding to the isotopically averaged species) of a possible drug-mediated conjugate would be neutral and not positively charged during the course of MS analysis. Were the peptide to be charged (very likely due to the acidic NH_4OAc work-up procedure employed for oligo mass spectral analysis) it is proposed that the lysines, arginines, the free N-terminus and the C-terminal amide could all be protonated thus affording a +8 charge on the peptide. This would result in an increase in mass of 8 units, thereby giving an expected mass of 12,729.3Da. More importantly, protonation of any one of these residues would enable the drug-mediated peptide–DNA cross-link to ion pair with acetate (an interaction not accessible to only native DNA). Such an interaction would increase the observed mass of the DNA–peptide cross-link by a factor of 59 per negatively charged OAc counterion. As such, potential masses of interest might be in the range of 12,781.3 Da (one positive charge on **BD 11** along with one acetate counterion) 12,841.3 Da (two positive charges both ion paired with OAc), 12,901.3 Da (three positive charges all ion paired with OAc) and so on. In line with this rationale, it is interesting to note that **BD 11** possesses 3 arginine groups each of which bears the extremely basic guanidine group. Protonation of each guanidine (preferential to the other amine functionalities within **BD 11**), followed by acetate ion-pairing would be expected to afford a drug-mediated DNA–peptide conjugate of mass 12,901.3 Da. Indeed the negative ion electrospray mass spectral analysis (Fig. 8) of the suspected conjugate afforded intense signals corresponding to masses of 12,899.1, 12,903.1, 12,906.0, and 12910.0 Da, all of which are well within the typical standard deviation of ±10 mass units. Notably, since ESI analysis of oligonucleotide adducts is performed under negative ion conditions, it is not surprising that a 'highest' mass signal corresponds to the peptide bearing a +3 charge as only the guanidines of **BD 11** could remain protonated during sample preparation. Thus, the results of ligand exchange and mass spectral analysis suggest, that the complex formed between **BD 11** and DNA substrates **12** and **12′** is in fact covalent and not due simply to enhanced non-covalent binding of the BD peptide to FR66979 alkylated DNA.

One concern with respect to mass spectral analysis of the peptide–DNA involved the generation of abasic sites within the substrate DNA thus altering the expected mass (and thus giving rise to the unidentifiable high mass species in Fig. 8). Additionally, the ability of an N^7 alkylated dG residue to undergo depurination and subsequent imine formation with a lysine on **BD 11** (Fig. 9) was an important consideration. Depurination has been shown to very efficiently induce DNA-histone cross-links via lysine addition to the resulting aldehyde of the abasic site (Fig. 9).[33] The ability of mitomycin C to induce abasic sites thus led to great concern regarding the nature of the FR66979 mediated cross-links. To probe this possible means of cross-linking and to determine the minor or major groove nature of the observed complex, piperidine digestion of the complexes formed between **BD 11** and both strands of template **A** was performed.

Isolation of both **ODN 12–BD 11** and **ODN 12′–BD 11** complexes was followed by 3′-end-labeling of each single-stranded species. Digestion of each complex in 1 M piperidine at 90 °C was expected to reveal any abasic lesions.[33] Examination of the resulting cleavage patterns (Fig. 10) revealed that peptide-bound DNAs did not undergo significant strand cutting over that seen in the piperidine control reactions. This suggests that the

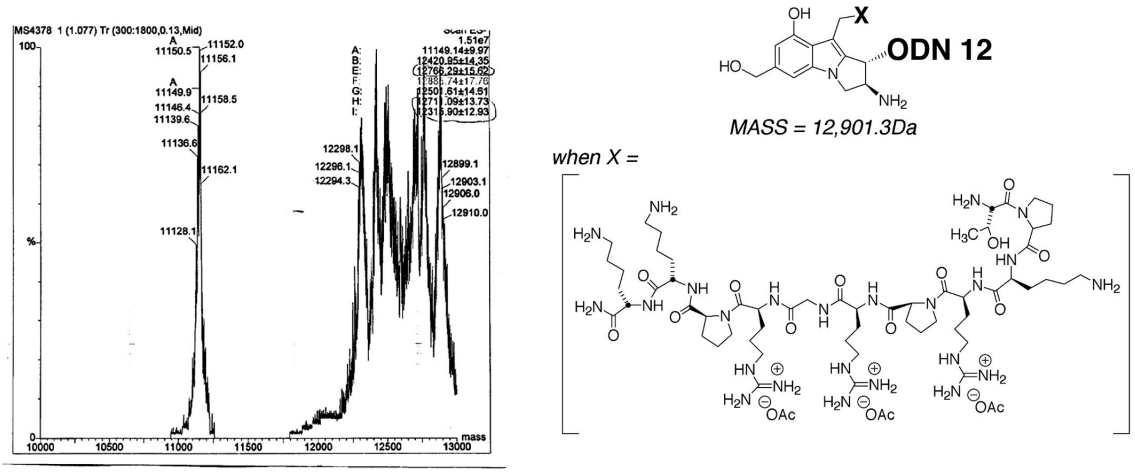

Figure 8. Negative ion electrospray mass spectral analysis of FR66979-mediated substrate **12-BD 11** cross-link. The signals to the left side of spectrum (mass range 11,128.1–11,122.1 Da) correspond to the parent mass for unmodified substrate **12** whereas the multiple signals in the range 12,294.3–12,910.0 Da correspond predominantly to unknown adducts. The signals from 12,899.1–12,910.0 Da are proposed to correspond to the +3 charged peptide–DNA adduct with each cationic species (from guanidine protonation) involved in ion-pairing with acetate as shown.

peptide–DNA lesion formed does not go through a depurination pathway since significant DNA cutting would have been observed at such a site. More importantly, this substantiates the anticipated minor groove nature of the drug-induced DNA–peptide cross-link and indicates that mass spectral analysis of these adducts is not likely to be complicated by sites of drug-induced depurination.

Conclusion

The only reported instance of HMG protein–DNA cross-linking to date involved the reaction of the binding domain of HMG 1 with cisplatin modified DNA.[29a] HMG 1 binds cisplatin modified DNA 100 times greater than normal DNA.[29a] Exploiting this high affinity ($K_b = 4\times10^7$M), Lippard and Kane showed that photolysis of the drug–DNA–protein complex afforded a DNA–protein cross-link which was reversible upon ligand exchange with NaCN or thiols. Photosubstitution of one of the ligands on Pt(II) (likely to be a purine involved in either inter- or intrastrand cross-linking) with Lys-6 of the HMG 1 binding domain is the proposed means by which protein attachment occurs.

Detailed herein is a synthetic DNA substrate, which upon monoalkylation by reductively activated FR66979, readily forms a DNA–peptide cross-link. This represents the first documented case of mitosene-based cross-linking of a DNA-binding peptide to a DNA substrate bearing the peptide recognition sequence.[28] Unlike the cisplatin case, little mechanistic information pertaining to FR66979 mediated DNA–protein cross-linking has been generated. The cross-link fails to undergo DNA exchange in the presence of competitor DNA and is resistant to denaturation at 90 °C for 3 min prior to denaturing gel electrophoresis. Negative ion electrospray mass spectral analysis reveals that a number of signals are obtained with some masses possibly corresponding to the tri-acetate salt of the FR66979-mediated DNA–peptide cross-link (wherein each guanidinium of

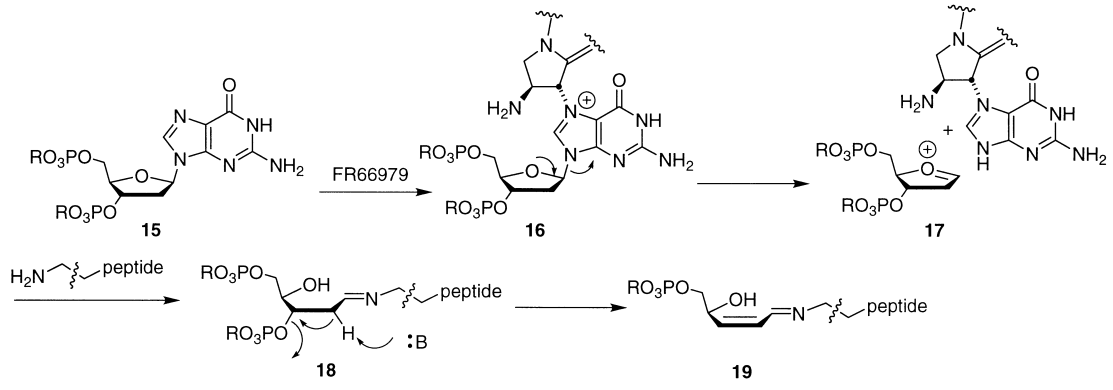

Figure 9. Proposed depurination route to DNA-peptide cross-linking by reductively activated FR66979.

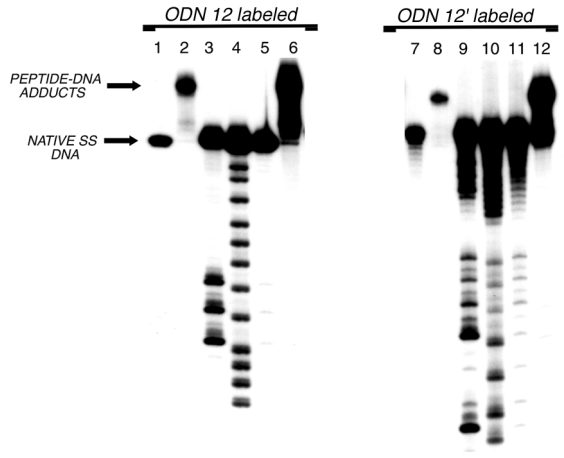

Figure 10. Piperidine digestion of FR66979-mediated **BD 11** complexes with 3′-labeled **ODN 12** and **ODN 12′**. Lane 1: standard template **A**:.Lane 2: **BD 11** complex with **ODN 12** control: Lanes 3,4: Maxam-Gilbert G, G + A respectively: Lane 5: 1M piperidine control reaction, Lane 6: **BD 11** substrate 12 complex subjected to 1M piperidine at 80 °C 30 min. Lanes 7–12: same as lanes 1–6 except using **ODN 12′**-bound **BD 11**.

BD 11 is ion-paired with acetate). As such, the proposed covalency of the mitosene-based cross-link has been supported. Additionally, the cross-link does not appear to operate via a depurination mechanism as piperidine digestion failed to render any base-labile lesions within the cross-linked DNA sequence. The relative biological importance of this finding as it relates to the tumor-selectivity of FR66979 and congeners is yet to be determined. However, given the preponderance of HMG-I(Y) proteins in rapidly proliferating undifferentiated cells, this may offer additional insights into how the mitomycins and related compounds exert biological activities which are selective for cancerous cell lines. The exact mechanism of this reaction has not yet been elucidated, and this, along with issues of regiochemistry, stereochemistry, sequence specificities, and the evaluation of this covalency in full-length HMG-I(Y) proteins both in vitro and in vivo is currently being examined in these laboratories.

Experimental

Materials and methods

FR900482 was generously supplied by the Fujisawa Pharmaceutical Co., Ltd., Japan. FR66979, FK973 were synthesized according to the Fujisawa patent Kokai 61-10590 and spectral data corroborated with the Fujisawa publication. All drug stock solutions were made up to 50 mM in sterile DDH_2O immediately prior to use, unless otherwise noted. Oligodeoxynucleotides were synthesized on an Applied Biosystems 380B DNA synthesizer using standard phosphoramidite chemistry (reagents and phosphoramidites from GLEN Research). Oligodeoxyribonucleotides (ODNs) were deprotected by heating 15 h at 55 °C in concentrated NH_4OH, followed by filtering of the CPG resin and concentration of supernatant in vacuo. All oligos were purified by 20% Denaturing Polyacrylamide Gel Electrophoresis (DPAGE). ODNs of interest were 5′ end-labeled with [γ-32P]ATP and T4 polynucleotide kinase (New England Biolabs) and then purified once more by 20% DPAGE. Labeled ODNs were then hybridized to their corresponding blunt ended complements in 200 mM Tris (pH = 7.5) by heating the equimolar mixture of oligodeoxynucleotides to 75 °C for 15 min then cooling to room temperature over 2 h then to 4 °C over another 2 h. 3′-End-labeling of DNA was performed using terminal deoxynucleotidyl transferase and α-32P-ddATP. Nucleotidyltransferase and ddATP were obtained from Amersham radiochemicals and reactions were run as per manufacturer's instructions. The 3′-end-labeled oligos were purified by Sephadex G-50 size exclusion chromatography and not 20% DPAGE. FeSO4 (from Mallinkrodt) solutions were made up to 4 mM using 4 mM EDTA 5 min before use. Mercaptoethanol (from Kodak) and dithiothreitol (from Gibco BRL) stock solutions were made using distilled deionized water immediately prior to use. Sodium acetate, tris, EDTA, and boric acid were also obtained from Gibco. DPAGE loading buffer contained 0.03% bromophenol blue, and 0.03% xylene cyanol in formamide. Dimethyl Sulfate and formic acid (88%) for Maxam-Gilbert sequence reactions were obtained from Mallinkrodt. Centrex MF 0.45 μm cellulose acetate spin filters were obtained from Schleicher & Schuell. Samples were counted on a Packard 1500 Tri-Carb liquid scintillation analyzer. All HMG BD peptides were prepared by solid phase synthesis by Macromolecular Resources (Dept. of Biochemistry, Colorado State University).

Precipitation of nucleic acids. Nucleic acids were routinely concentrated by precipitation with absolute ethanol. Precipitation was carried out by adjustment of the concentration of monovalent cations (NaOAc, pH 5.2) in the nucleic acid solution to 0.3 M final and the addition of 3 volumes of ethanol. The contents were well mixed by either inversion and shaking of the Eppendorf tube containing the ethanolic solution or by vortexing for 30 s at high speed. The mixture was then placed in dry ice acetone bath (−78 °C) for 15 min followed by centrifugation at 14,000 rpm at 4 °C for 12 min. The supernatant was carefully removed with a 0–200 μL sized Eppendorf pipetman and the remaining DNA pellet dried in vacuo. The nucleic acid was then redissolved in either DDH_2O or an appropriate buffer.

Quantitation of DNA. Pure samples of DNA (typically after 20% denaturing polyacrylamide gel electrophoresis and subsequent extraction/isolation) were quantitated by measuring the absorbance at 260 nm using a UV spectrophotometer. Molar extinction coefficients for the ODNs of interest were calculated using the nearest neighbor method described by Borer[34] in conjunction with optical density measurements obtained by ultraviolet absorption at 260 nm. Notably, quantitation of radiolabeled DNA in this fashion was not possible via UV spectrophotometric means. Quantitation of these ODNs was obtained by liquid scintillation of a given sample and comparison to the starting material's activity.

Maxam-Gilbert G reactions. 5′ or 3′ end-labeled samples of DNA (typically 1 μg) were dissolved into 10 μL ddH_2O and to each sample was added 200 μL of Maxam–Gilbert G reaction buffer. To each 210 μL sample of DNA was added 1 μL of dimethyl sulfate (DMS) at room temperature. Each sample was aged at room temperature for 7–9 min followed by the addition of 750 μL absolute EtOH, 10 μL tRNA (1 mg/mL stock solution), and 30 μL 3 M NaOAc (pH = 5.2). Reactions were kept at −80 °C for 15 min and centrifugation at 14,000 RPM carried out at 4 °C for 10 min. The supernatant was discarded and the remaining pellet dissolved in 100 μL ddH_2O followed by another EtOH precipitation (w/o tRNA addition). Following centrifugation the pellet was removed from the supernatant and the EtOH precipitation procedure repeated once more to ensure complete removal of G-reaction buffer salts. The pellet was dried in vacuo. To the pellet was added 100 μL 0.8 M piperidine (prepared immediately prior to use) and the mixture heated to 80–90 °C for 20 min. The sample was then placed at −80 °C and lyophilized to dryness. To the lyophilate was then added 100 μL ddH_2O and the lyophilization procedure repeated. Samples were dissolved in 50 μL DPAGE loading dye and the activity of each sample determined by liquid scintillation. Final activities of G reactions ranged from 2000 to 8000 cpm/μL.

Maxam-Gilbert G + A reactions. The 5′- or 3′-end-labeled samples of DNA (typically 1 μg) were dissolved into 10 μL ddH_2O and to each sample was added 10 μL of ddH_2O. To each 20 μL sample of DNA was added 50 μL of formic acid (88%) at room temperature. Each sample was aged at room temperature for 7–9 min followed by the addition of 220 μL absolute EtOH, 10 μL tRNA (1 mg/mL stock solution), and 15 μL 3 M NaOAc (pH = 5.2). Reactions were kept at −80 °C for 15 min. and centrifugation at 14,000 RPM carried out at 4 °C for 10 min. The supernatant was discarded and the remaining pellet dissolved in 100 μL ddH_2O followed by another EtOH precipitation (w/o tRNA addition). Following centrifugation the pellet was removed from the supernatant and the EtOH precipitation procedure repeated once more. The pellet was dried in vacuo. To the pellet was added 100 μL of 1 M piperidine solution (prepared immediately prior to use) and the mixture heated to 80–90 °C for 20 min. The sample was then placed at −80 °C and lyophilized to dryness. To the lyophilate was then added 100 μL ddH_2O and the lyophilization procedure repeated. Samples were dissolved in 50 μL DPAGE loading dye and the activity of each sample determined by liquid scintillation. Final activities of G + A reactions ranged from 2000 to 12,000 cpm/ μL.

Recovery of radiolabeled DNAs from DPAGE (crush and soak method). Unless otherwise noted, all radiolabeled DNAs/DNA adducts were isolated as follows. Following drug and/or peptide reactions, samples were typically EtOH precipitated and then redissolved in a 1:1 mixture of ddH_2O and DPAGE loading dye. Using analytical thickness (0.4 mm) 10% DPAGE, the samples were loaded to an appropriate number of wells (20 μL maximum volume per well) and electrophoresis carried out at 50–75 Watts. Electrophoresis was traditionally carried out until the xylene cyanol dye (the slower mobility of the two dyes) was within 10 cm of the gel bottom. The gel was removed from the apparatus and the plates separated so as to render the gel on only one plate. The gel was wrapped with plastic wrap and a clean glass plate placed on top so as to shield radiation. Once in the darkroom, the top glass plate was removed and a piece of Kodak BioMax X-ray film placed on top of the gel. The top glass plate was placed on top of the X-ray so as to not completely cover the exposed gel surface. Using the top glass plate as a template, a razor blade was used to place cuts through both the X-ray and the gel below. Typical exposure times ranged from 2 to 5 min, after which time the X-ray was developed, rinsed with ddH_2O and then wiped dry. The bands of interest were cut out of the X-ray image. The slash marks through the X-ray and the gel were aligned and the band of interest excised from the gel using the X-ray as the template. DNAs were finely crushed using a glass rod and then eluted into 3–5 mL of 500 mM NH_4OAc/ 1 mM EDTA at 37 °C for 1 h. It is noteworthy that efficient elution (≥80% recovery) may be achieved from 10% DPAGEs at room temperature in 10 min with occasional vortexing. Following elution, the crushed acrylamide matter was filtered off using centrex 0.45 μm centrifugation filters (VWR Scientific). The eluant was butanol extracted to a volume of 200–300 μL and then EtOH precipitated as described earlier.

Piperidine digestion of DNAs (controls and alkylated adducts). DNAs (typically 1–3 μg of radiolabeled material) were EtOH precipitated from ddH_2O at least one time so as to ensure minimal salt content. Samples were then dried in vacuo and resuspended into 100 μL 1M piperidine (prepared via 1:9 aqueous dilution of commercially available piperidine). Samples were rigorously vortexed for 2 min and then heated 80–90 °C for 30 min with occasional vortexing. The samples were then withdrawn from the heating block and placed in dry ice for 1 min and centrifuged so as to get all liquid into the bottom of the 1.7 mL Eppendorf tube. Samples were frozen completely solid at −80 °C and then a small hole melted into the top of the Eppendorf tube. Samples were lyophilized to dryness (typically 12 h) and then resuspended into 100 μL of ddH_2O and the freezing/ lyophilization process repeated once more. Following the second lyophilization, samples were resuspended into 20 μL DPAGE loading dye and 10–20 μL of this solution was transferred to a fresh tube. Samples were counted by liquid scintillation and then brought to an activity of 1000–3000 cpm/μL.

FR66979-mediated DNA–peptide cross-linking of template A and HMG BD peptide BD 11 (Fig. 6). To 10 nmoles of 5′-^{32}P-end-labeled oligos **ODN 12** and **ODN 12′** annealed to their correspondingly unlabeled complements was added 100 μL 200 mM Tris (pH = 7.5). This resulted in stock solutions 0.1 mM in template **A**. The ODNs were annealed as described previously and then divided into two 50 μL aliquots. To one 50 μL aliquot for each differently radiolabeled duplex was added 50 mM FR66979 and 2M DTT to final concentrations of 10 mM drug and 100 mM thiol. To the

other 50 μL batches of each duplex was added ddH_2O instead of drug. The same volume of thiol was added so as to achieve a final concentration of 100 mM DTT. Reactions were incubated at 25 °C for 12 h after which time the reactions were passed through a Sephadex G-50 size exclusion column and the first radioactive fraction of each reaction collected and EtOH precipitated. The pellets were resuspended into 100 μL ddH_2O once more and EtOH precipitated once more to ensure desalting. The samples were then dried in vacuo and then resuspended into 250 μL 10 mM Tris (pH = 8.0). This afforded stock solutions of FR66979 modified DNA 20 μM in duplex (740 μM in base pairs). The following DNA–peptide reactions were set up at room temperature and allowed to incubate 37 °C for 12–24 h. These reactions were done in glass-lined screw top autosampler vials (100 μL volume) due to the known tendency of the peptide to adhere to the inside of plastic eppendorf tubes. Following 37 °C incubation, 5 μL aliquots were withdrawn from each reaction and added to 15 μL of DPAGE dye. Samples were then analysed by 20% DPAGE. It is noteworthy that whether or not the samples were heated to 90 °C for 3 min prior to loading did not affect the amount of gel retarded material in the peptide + drug reactions. To ensure denaturation, samples were typically loaded and the gel faceplate heated with a heat gun during the first 5 min of electrophoresis (Table 1).

Ligand exchange reactions of ODN 12 and ODN 12′ drug-mediated complexes with BD 11 (Fig. 7). The entire reaction contents from the experiment above were added to an equal volume of DPAGE loading dye and then loaded to an analytical thickness 20% DPAGE. The DNAs 0.4 mm above the gel-shifted bands were purified as described previously and then subjected to re-labeling with terminal deoxynucleotidyl transferase and α-^{32}P-ddATP. The radiolabeled bands were then EtOH precipitated, resuspended and passed through a Sephadex G-50 column. The first radiolabeled fractions were collected and EtOH precipitated. It is particularly noteworthy that these bands did not contain the 5′-end-labeled material as this would interfere with later sequencing methods. Additionally, single-stranded 3′-end-labeled **ODN 12** and **ODN 12′** were purified on the same gel and used as standards. Each gel-shifted ODN was then dissolved into 100 μL ddH_2O. From each peptide–DNA complex was then withdrawn 10 μL and using these aliquots, the following reactions (Table 2) with unlabeled duplex competitor template **A** set up. All reactions were approximately 0.2 μM in peptide–DNA complex. This value was based on the fact that each reaction in the preceeding section contained 20 μl of a 20 pmol/μL DNA solution. From each reaction was obtained about 10% (by LSC) yield of the DNA-peptide conjugate. This would equate to 40 pmol of the gel-shifted material. After radiolabeling and purification, this complex was resuspended into 100 μl ddH_2O thus affording 0.4 pmol of complex per μl. Ten μl of this solution could afford 4 pmol to be ultimately dissolved in a total of 20 μl for each 'exchange' reaction. In short, each ODN-peptide stock solution was 0.4 μM. All exchange reactions were incubated 37 °C for 24 h after which time 5 μl aliquots were withdrawn and placed in 10 μl DPAGE dye. Samples were heated 90 °C 2 min prior to DPAGE analysis. 20% DPAGE analysis was carried out similarly to that described above to yield the image in Figure 7.

Table 1. Reactions of FR66979 alkylated template **A** with HMG peptide **BD 11**

Entry/reaction	μL FR66979 modified template **A**[a]	μL HMG peptide **BD 11**	μL ddH_2O
1	20 (ODN 12′)	—	20
2	20 (ODN 12′)	20 (100 μM)	—
3	20 (ODN 12′)	—	20
4	20 (ODN 12′)	20 (100 μM)	—
5	20 (ODN 12)	—	20
6	20 (ODN 12)	20 (100 μM)	—
7	20 (ODN 12)	—	20
8	20 (ODN 12)	20 (100 μM)	—

[a]ODN in parentheses denotes which strand of template **A** was radiolabeled. Other parentheses values denote stock solution concentration.

Mass spectral analysis of FR66979 mediated ODN 12 and ODN 12′ complexes with BD 11 (Fig. 8). To 100 nmoles of **ODN 12** (unlabeled) was added 100 nmoles of **ODN 12′** The oligos were EtOH precipitated as described earlier and then dried in vacuo. Resuspension into 1 mL of 200 mM Tris (pH = 7.5) was performed and the strands annealed to each other by heating to 80 °C 10 min and then cooling to room temperature over the course of a 2 h. To the resulting duplex was added 50 mM FR66979 and 2M DTT so as to afford a final concentration of 10 mM FR66979 and 100 mM DTT. Reactions were kept at room temperature for 24 h and the samples then EtOH precipitated. Resulting pellets were resuspended in 100 μL ddH_2O and EtOH precipitation effected once again. This cycle was performed once more and the sample then dried in vacuo. The presumably alkylated species was then resuspended into 5 mL 10 mM Tris (pH = 8.0) so as to afford a stock solution of 20 pmol/μL. To 4.5 mL. of this solution was added an equal volume of 0.1 mM **11** in ddH_2O. To the remaining 0.5 mL of DNA was added an equal volume of ddH_2O. Both reactions were heated 37 °C for 24 h followed by cooling to 4 °C and subsequent butanol extraction down to a volume of 500 μL. To each 500 μL batch was added an equal volume of DPAGE dye and the samples loaded to a preparative 20% DPAGE. Samples were then worked up as described above. Negative ion electrospray mass spectral analysis yielded the image depicted by Figure 8.

Piperidine digestion of FR66979 mediated ODN 12 and ODN 12′ complexes with BD 11 (Fig. 10). Using the remainder of the gel-shifted complexes obtained immediately above, piperidine digestions were set up. 30 μL of each complex was lyophilized to dryness to each was then added 100 μL 1M piperidine. Analagous control digestions were run alongside the peptide reactions. Samples were heated and then worked up as previously described. Following lyophilization each sample was resuspended into 10 μL DPAGE dye, transferred to a new eppendorf tube and counted by LSC. Samples were

Table 2. Reaction volumes and concentrations of DNA-exchange reactions of **ODN 12**/**ODN 12′** complexes with **BD 11** and unlabeled duplex template **A**[a]

Entry/reaction	μL **BD 11**-DNA complex	μL 'cold' template A	μL10 mM Tris	['cold' template A] (μM)	% retention of gel-shift adduct[a]
1	10 (ODN 12)	—	10	—	N/A
2	10 (ODN 12)	—	10	—	74.6
3	10 (ODN 12)	10 (0.5 μM)	—	0.25	62.4
4	10 (ODN 12)	10 (5 μM)	—	2.5	77.4
5	10 (ODN 12)	10 (50 μM)	—	25	74.4
6	10 (ODN 12)	10 (500 μM)	—	250	75.8
7	10 (ODN 12′)	—	10	—	N/A
8	10 (ODN 12′)	—	10	—	65.0
9	10 (ODN 12′)	10 (0.5 μM)	—	0.25	64.8
10	10 (ODN 12′)	10 (5.0 μM)	—	2.5	67.7
11	10 (ODN 12′)	10 (50 μM)	—	25	70.0
12	10 (ODN 12′)	10 (500 μM)	—	250	66.7

[a]Values in parentheses denote stock solution concentrations. In the case of the **BD 11**-DNA complexes, the parentheses denote which complex was used. Values based on band excision and subsequent liquid scintillation counting.

then brought to an activity of 1000 cpm/μL. Standards for both native DNA and peptide complexes were brought to an activity of 725 cpm/μL, while G and G + A lanes were brought to activities of 1000, and 2000 cpm/μl respectively. The activities loaded to gels depicted in Figure 10 are as follows: DNA and DNA–peptide controls: 725 cpm/well, Maxam–Gilbert G: 2000 cpm/well, G + A: 4000 cpm/well, all piperidine reactions 3000 cpm/well. Electrophoresis was carried out at 60 W for 3.5 h. Autoradiography was then conducted at −80 °C for 14 h to afford the image in Figure 10. Notably, no prominent base labile sites were seen in peptide-containing digestions that did not appear in control digestions.

Acknowledgements

This work was supported by the National Institutes of Health (CA51475). We are indebted to Fujisawa Pharmaceutical Corporation of Japan for the gift of authentic FR900482 from which FR66979 was prepared by reduction. The authors wish to acknowledge Professor Marc Greenberg (Colorado State University) for use of liquid scintillation facilities. We are also indebted to reviewers of this manuscript for thoughtful and constructive comments.

References and Notes

1. Lawley, P. D. *Bioessays* **1995**, *17*, 561.
2. Paustenbach, D. J.; Finley, B. L.; Kacew, S. *Proc. Soc. Exp. Biol. Med.* **1996**, *211*, 211.
3. Rajski, S. R.; Williams, R. M. *Chem. Rev.* **1998**, *98*, 2723.
4. Bridgewater, L. C.; Manning, F. C. R.; Patierno, S. R. *Carcinogenesis* **1994**, *15*, 2421.
5. (a) Sancar, A. *Annu. Rev. Biochem.* **1996**, *65*, 43. (b) Lawley, P. D.; Lethbridge, J. H.; Edwards, P. A.; Shooter, K. V. *J. Mol. Biol.* **1969**, *39*, 181.
6. (a) Iwami, M.; Kiyoto, S.; Terano, H.; Kohsaka, M.; Aoki, H.; Imanaka, H. *J. Antibiotics* **1987**, *40*, 589. (b) Kiyoto, S.; Shibata, T.; Yamashita, M.; Komori, T.; Okuhara, M.; Terano, H.; Kohsaka, M.; Aoki, H.; Imanaka, H. *J. Antibiotics*, **1987**, *40*, 594. (c) Uchida, I.; Takase, S.; Kayakiri, H.; Kiyoto, S.; Hashimoto, M.; Tada, T.; Koda, S.; Morimoto, Y. *J. Am. Chem. Soc.* **1987**, *109*, 4108.
7. (a) Shimomura, K.; Hirai, O.; Mizota, T.; Matsumoto, S.; Mori, J.; Shibayama, F.; Kikuchi, H. *J. Antibiotics*, **1987**, *40*, 600. (b) Hirai, O.; Shimomura, K.; Mizota, T.; Matsumoto, S.; Mori, J.; Kikuchi, H. *J. Antibiotics* **1987**, *40*, 607. (c) Masuda, K.; Makamura, T.; Shimomura, K.; Shibata, T.; Terano, H.; Kohsaka, M. *J. Antibiotics* **1988**, *41*, 1497. (d) Masuda, K.; Nakamura, T.; Mizota, T.; Mori, J.; Shimomura, K. *Cancer Res.* **1988**, *48*, 5172.
8. Terano, H.; Takase, S.; Hosoda, J.; Kohsaka, M. *J. Antibiotics* **1989**, *42*, 145.
9. (a) Shimomura, K.; Manda, T.; Mukumoto, S.; Masuda, K.; Nakamura, T.; Mizota, T.; Matsumoto, S.; Nishigaki, F.; Oku, T.; Mori, J.; Shibayama, F. *Cancer Res.* **1988**, *48*, 1166. (b) Nakamura, T.; Masuda, K.; Matsumoto, S.; Oku, T.; Manda, T.; Mori, J.; Shimomura, K. *Japan. J. Pharmacol.* **1989**, *49*, 317.
10. (a) Naoe, Y.; Inami, M.; Matsumoto, S.; Nishigaki, F.; Tsujimoto, S.; Kawamura, I.; Miyayasu, K.; Manda, T.; Shimomura, K. *Cancer Chemother. Pharmacol.* **1998**, *42*, 31. (b) Naoe, Y.; Inami, M.; Kawamura, I.; Nishigaki, F.; Tsujimoto, S.; Matsumoto, S.; Manda, T.; Shimomura, K. *Jpn. J. Cancer Res.* **1998**, *89*, 666. (c) Naoe, Y.; Inami, M.; Takagaki, S.; Matsumoto, S.; Kawamura, I.; Nishigaki, F.; Tsujimoto, S.; Manda, T.; Shimomura, K. *Jpn. J. Cancer Res.* **1998**, *89*, 1047. (d) Naoe, Y.; Inami, M.; Matsumoto, S.; Takagaki, S.; Fujiwara, T.; Yamazaki, S.; Kawamura, I.; Nishigaki, F.; Tsujimoto, S.; Manda, T.; Shimomura, K. *Jpn. J. Cancer Res.* **1998**, *89*, 1306. (e) Naoe, Y.; Kawamura, I.; Inami, M.; Matsumoto, S.; Nishigaki, F.; Tsujimoto, S.; Manda, T.; Shimomura, K. *Jpn. J. Cancer Res.* **1998**, *89*, 1318. For recent results of the Phase I clinical trials of FK317, see: (f) Furuse, K.; Hasegawa, K.; Kudo, S.; Niitaru, H. *Proc. Am. Soc. Clin. Oncol.,* **1999**, *18*, 179a. (abstract #689). (g) Ravandi, F.; Wenske, C.; Royca, M.; Hoff, P.; Brito, R.; Zukowski, T.; Mekki, Q.; Pazdur, R. *Proc. Am. Soc. Clin. Oncol.* **1999**, *18*, 225a, (abstract #867).
11. (a) Tomasz, M; Lipman, R.; Chowdary, D.; Pawlak, J.; Verdine, G.; Nakanishi, K. *Science*, **1987**, *235*, 1204; (b) Tomasz, M. *Chem. Biol.* **1995**, *2*, 575 and references cited therein.
12. (a) Iyengar, B. S.; Door, R. T.; Remers, W. A.; Kowal, C. D. *J. Med. Chem.* **1988**, *31*, 1579. (b) Remers, W. A.,; Rao, S. N.; Wunz, T. P.; Kollman, P. A. *J. Med. Chem.* **1988**, *31*, 1612. (c) Iyengar, B. S.; Remers, W. A.; Catino, J. J. *J. Med. Chem.* **1989**, *32*, 1866. (d) E. O.; Verboom, W.; Scheltinga, M. W.; Reinhoudt, D. N.; Lelieveld, P.; Fiebig, H. H.; Winterhalter,

B. R.; Double, J. A.; Bibby, M. C. *J. Med. Chem.* **1989**, *32*, 1612. (e) Tomasz, M.; Lipman, R.; Snyder, J. K.; Nakanishi, K. *J. Am. Chem. Soc.* **1983**, *105*, 2059. (f) Tomasz, M.; Lipman, R.; Verdine, G.; Nakanishi, K. *Biochemistry*, **1986**, *25*, 4337. (g) Verdine, G. L.; McGuinness, B. F.; Nakanishi, K.; Tomasz, M. *Heterocycles*, **1987**, *25*, 577. (h) McGuinness, B.; Nakanishi, K.; Lipman, R.; Tomasz, M. *Tetrahedron Lett.* **1988**, *29*, 4673. (i) Hashimoto, Y.; Shudo, K.; Okamoto, T. *Tetrahedron Lett.* **1982**, *23*, 677. (j) Zein, N.; Kohn, H. *J. Am. Chem. Soc.* **1987**, *109*, 1576; (k) Zein, N.; Kohn, H. *J. Am. Chem. Soc.* **1986**, *108*, 296. (l) Egbertson, M.; Danishefsky, S. J. *J. Am. Chem. Soc.* **1987**, *109*, 2204. (m) Kohn, H.; Hong, Y. P. *J. Am. Chem. Soc.* **1990**, *112*, 4596. (n) Millard, J. T.; Weidner, M. F.; Raucher, S.; Hopkins, P. B. *J. Am. Chem. Soc.* **1990**, *112*, 3637. (o) Sartorelli, A. C.; Pristos, C. A. *Cancer Research*, **1986**, *46*, 3528.

13. (a) Williams, R. M.; Rajski, S. R. *Tetrahedron Lett.* **1992**, *33*, 2929. (b) Williams, R. M.; Rajski, S. R. *Tetrahedron Lett.* **1993**, *34*, 7023. (c) Huang, H.; Rajski, S. R.; Williams, R. M.; Hopkins, P. B. *Tetrahedron Lett.* **1994**, *35*, 9669.

14. (a). Huang, H.; Pratum, T. K.; Hopkins, P. B. *J. Am. Chem. Soc.* **1994**, *116*, 2703. (b) Woo, J.; Sigurdsson, S. Th.; Hopkins, P. B. *J. Am. Chem. Soc.* **1993**, *115*, 1199. (c) Paz, M. M.; Hopkins, P. B. *Tetrahedron Lett.* **1997**, *38*, 343; (d) Paz, M. M.; Hopkins, P. B. *J. Am. Chem. Soc.* **1997**, *119*, 5999.

15. Williams, R. M.; Rajski, S. R.; Rollins, S. B. *Chem. Biol.* **1997**, *4*, 127.

16. Kim, H. Y.; Stermitz, F. R.; Coulombe, R. A. *Carcinogenesis* **1995**, *16*, 2691.

17. For excellent reviews see: (a) Pabo, C. O.; Sauer, R. T. *Ann. Rev. Biochem.* **1992**, *61*, 1053. (b) Takeda, Y.; Ohlendorf, D. H.; Anderson, W. F.; Matthews, B. W. *Science*, **1983**, *221*, 1020. (c) Travers, A. *Annu. Rev. Biochem.* **1989**, *58*, 427. (d) Seeman, N. C.; Rosemberg, J. M.; Rich, A. *Proc. Natl. Acad. Sci. USA* **1976**, *73*, 804.

18. (a) Neidle, S. O. *FEBS* **1992**, *298*, 97. (b) Turnell, W. G.; Satchwell, S. C.; Travers, A. A. *FEBS,* **1988**, *232*, 263.

19. Eckner, R.; Birnstiel, M. L. *Nucleic Acids Research* **1989**, *17*, 5947.

20. (a) Reeves, R.; Nissen, M. S. *J. Biol. Chem.* **1990**, *265*, 8573. (b) Reeves, R.; Langan, T. A.; Nissen, M. S. *Proc. Nat. Acad. Sci. USA* **1991**, *88*, 1671.

21. Grosschedl, R.; Giese, K.; Pagel, J. *Trends Genetics*, **1994**, *10*, 94.

22. (a) Du, W.; Thanos, D.; Maniatis, T. *Cell*, **1993**, *74*, 887. (b) Thanos, D.; Maniatis, T. *Cell*, **1992**, *71*, 777.

23. Siino, J. S.; Nissen, M. S.; Reeves, R. *Biochem. Biophys. Res. Comm.* **1995**, *207*, 497.

24. Evans, J. N. S.; Zajicek, J.; Nissen, M. S.; Munske, G.; Smith, V.; Reeves, R. *Int. J. Peptide Protein Res.* **1995**, *45*, 554.

25. Reeves, R.; Wolffe, A. P. *Biochemistry* **1996**, *35*, 5063.

26. Geierstanger, B. H.; Volkman, B. F.; Kremer, W.; Wemmer, D. E. *Biochemistry* **1994**, *33*, 5347.

27. For additional citations petinent to Asx turns see: (a) Imperiali, B.; Spencer, J. R.; Struthers, M. D. *J. Am. Chem. Soc.* **1994**, *116*, 8424. (b) Abbadi, A.; Mcharfi, M.; Premilat, S.; Boussard, G.; Marraud, M. *J. Am. Chem. Soc.* **1991**, *113*, 2729. (c) Aubry, A.; Abbadi, A.; Boussard, G.; Marraud, M. *New Journal of Chemistry* **1987**, *11*, 739.

28. For a preliminary account of this work, see: Rajski, S. R.; Rollins, S. B.; Williams, R. M. *J. Am. Chem. Soc.* **1998**, *120*, 2192

29. Of particular interest, is the recent report by Lippard on the cisplatin-HMG1-DNA cross-link: (a) Kane, S. A.; Lippard, S. J. *Biochemistry* **1996**, *35*, 2180. (b) Sancar, A.; Hearst, J. H.; Sastry, S. S.; Spielmann, P. H.; Hoang, Q. S. *Biochemistry* **1993**, *32*, 5526. (c) Farrell, N.; Appleton, T. G.; Qu, Y.; Roberts, J. D.; Soares-Fontes, A. P.; Skov, K. A.; Wu, P.; Zou, Y. *Biochemistry* **1995**, *34*, 15480.

30. Huth, J. R.; Bewley, C. A.; Nissen, M. S.; Evans, J. N. S.; Reeves, R.; Gronenborn, A. M.; Clore, G. M. *Nature Struct. Biol.* **1997**, *4*, 657.

31. Coordinates for the PRGRP fragment of HMG I/Y bound to the recognition sequence 5′-AATT-3′ were courtesy of Professor D. Wemmer (UC Berkeley).

32. It should be noted that addition of a 2% Triton X-100 aqueous solution to the reactions did not significantly improve the recovery of radiolabeled DNA–protein adducts.

33. The susceptibility towards β-elimination of the peptidic Schiff base formed with apurinic sites upon digestion with piperidine is supported by: (a) Singh, M. P.; Hill, C. G.; Peoc'h, D.; Rayner, B.; Imbach, J. L.; Lown, W. J. *Biochemistry* **1994**, *33*, 10271; and (b) Bailly, V.; Verly, W. G. *Biochem. J.* **1988**, *253*, 553.

34. Borer, P. N. *Handb. Biochem. Mol. Biology*. CRC Press, 1975.